Simultaneous photocatalytic reduction/degradation of divalent nickel/naphthalene pollutants in aqueous solutions

Javad Saien, Amir Azizi and Fatemeh Ghamari

ABSTRACT

Toxic heavy metals and organic pollutants simultaneously exist in the wastewater of some industries. This study explores reduction of toxic divalent nickel ions, from either nitrate or sulfate salts, coupled with naphthalene (NA) degradation using titania photocatalyst in an efficient photo-sono reactor. A synergism appears when reduction and degradation treatments occur simultaneously in the media. With initial concentrations of $[Ni(II)]_0 = 5$ mg/L and $[NA]_0 = 10$ mg/L, under dominant mild conditions, removal efficiencies of 54.5% and 56.6% were obtained for Ni(II) and NA, respectively, when nickel nitrate was used. These efficiencies were enhanced to 59.2% and 57.5%, respectively, with nickel sulfate, all after 90 min operation. For evaluating the mechanism of reactions, reactive oxygen species analysis on solutions as well as Fourier transform infrared, scanning electron microscopy and Brunauer–Emmett–Teller analyses on the titania nanoparticles, before and after usage, was performed. The reaction kinetics was also followed for individual species in the mixed solution and, accordingly, the energy consumption was evaluated for one order of magnitude decrease in pollutant concentration. The high performance of the used method was revealed in comparison to the similar reported reduction/degradation processes.

Key words | divalent nickel, energy consumption, kinetics, naphthalene, photocatalytic treatment

Javad Saien (corresponding author)
Fatemeh Ghamari
Faculty of Chemistry,
Bu-Ali Sina University,
65178-38683 Hamedan,
Iran
E-mail: *saien@basu.ac.ir*

Amir Azizi
Department of Chemistry, Faculty of Science,
Arak University,
Arak 3815688138,
Iran

INTRODUCTION

Pollution of water and wastewaters by toxic heavy metals and organic compounds has been a major concern during recent decades. Among heavy metals, nickel is one of the potentially toxic metals, which has many applications in important industries such as stainless steel, nickel alloy, storage battery and electroplating (Joshi *et al.* 2011). Although Ni(II) has been identified as a component for participating in important metabolic reactions such as ureolysis, acidogenesis and methane biogenesis (Akhtar *et al.* 2004), but human contact with excessive amount of this ion can cause problems from skin irritation to lung damage and mal effects on the nervous system and mucous membranes (Caicedo 2008). In aquatic environments, nickel appears as Ni(II) and zero-valent Ni^0; however, the potential toxicity for Ni(II) is reported as high whereas Ni^0 is only slightly toxic (Chen & Ray 2001). The World Health Organization (WHO) recommends maximum concentration of nickel not to exceed 0.5 mg/L in waters (WHO 2008). Thus, reduction of Ni(II) to less harmful species would be very beneficial. Further, wastewaters from industries like electroplating usually contain organic compounds, which are used in different stages of manufacturing processes as balms, ductile material, polisher and so on. Naphthalene (NA), for instance, is widely used in different metal industries as brightener (Doan & Saidi 2008).

Several methods have been reported to treat wastewaters containing heavy metals and other pollutants. Ion exchange, membrane separation, adsorption, coagulation, electrolysis, and chemical precipitation are noteworthy. At the same time, it has been pointed out that these methods are coincident with some disadvantages including secondary pollution, large quantities of chemical reagents, high cost, poor treatment efficiency at low pollutant concentration and high energy consumption (Akhtar *et al.* 2004; Alqadami *et al.* 2017; Naushad *et al.* 2017).

A promising alternative is using advanced oxidation processes (AOPs) for pollutants removal due to high efficiency, wide adaptability and potential for simultaneous

doi: 10.2166/wst.2019.022

treatment of different pollutants (Saravanan *et al.* 2018). Among AOPs, heterogeneous photocatalysis by using semiconductors has been demonstrated with great success for the reduction of toxic metals as well as oxidation of organic compounds (Wang *et al.* 2004).

Upon irradiation of the semiconductor–solution interface with light energies greater than the semiconductor band gap, electron–hole pairs ($e^-_{CB} - h^+_{VB}$) are formed in the photocatalyst conduction and valence bands, respectively (Barakat 2004). The electron–hole pairs are then separated and the adsorbed species on the sites of the catalyst undergo photo-induced redox reactions. For this aim, titania has been known as a very efficient photocatalyst since its band gap is around 3.2 eV with conduction band (CB) energy of −0.3 eV and valence band of +2.9 eV at pH 5.6 (Blake *et al.* 1991). Thus, any metal ion with a reduction potential less negative than −0.3 eV will be potentially reduced by photo-generated electrons of TiO_2. Also, the photocatalytic process, under aerobic conditions, can generate several reactive oxygen species (ROS) including superoxide anion radical hydroxyl and hydrogen peroxide through reactions with dissolved oxygen (DO) (Nosaka & Nosaka 2017). The ROS contribute in the oxidation and reduction reactions.

A variety of methods for simultaneous photocatalytic reduction of heavy metals and degradation of organic compounds have been proposed. For instance, the photoreduction of Cu(II) and Se(IV) in the presence of formic acid and ethylene diamine tetra-acetic acid (EDTA) was investigated by Aman *et al.* (2011). Simultaneous Cr(VI) reduction and NA degradation in aqueous solutions by UV/TiO_2 has been investigated in another work by Gutierrez *et al.* (2008). A synergic effect between Cr(VI) reduction and NA degradation by UV/TiO_2 process was reported. In our recent study, simultaneous photocatalytic reduction of Cr(VI) and Ni(II) ions, coupled with degradation of sodium dodecyl benzene sulfonate, was reported (Saien & Azizi 2015). Enhanced photocatalytic treatment of pollutants is of interest due to a low dosage of titania nanoparticles and mild operating conditions.

Here, an attempt was made for the first time, for the photocatalytic reduction of nickel ions originating from nitrate or sulfate salts and in the presence of NA. The nitrate and sulfate salts are often present in the wastewaters of some industries like petroleum refining, electroplating, petrochemical, dyeing, textile and steel manufacturing (Ashour *et al.* 2008; Besharat 2010). NA, on the other hand, is extensively used as brightener and ductile agent in the nickel electroplating industries (Doan & Saidi 2008; Besharat 2010). Experiments were conducted in an efficient photo-sono reactor working with UV irradiation. For practical applications, the process performance was evaluated in terms of reaction kinetics, energy consumption and a specified process efficiency.

MATERIALS AND METHODS

Chemicals

All the used chemicals, including nickel nitrate hexa-aqua (98.5%), nickel sulfate hexa-aqua (99%), 1-(2-pyridylazo)-2-naphthol (PAN) (>99%), ethanol (99.9%) and Triton X-100, naphthalene (99%), sulfuric acid (98%), sodium nitrate (98.9%), sodium sulfate (99%), potassium iodine (99.8%), sodium acetate (99%), ammonium dimolybdate (>99%) and sodium hydroxide (>97%), were purchased from Merck. Titanium dioxide nanosize particles, P-25 (>99.5%), was an Evonik product (anatase to rutile weight ratio of about 80/20) with Brunauer–Emmett–Teller (BET) surface area of 50 ± 15 m^2/g and average particle diameter of 21 nm. All aqueous solutions were prepared using deionized water with conductivity of less than 0.08 μS/cm.

Photo reactor and experimental procedure

A 1.25 L cylindrical photo-sono reactor made of glossy stainless steel with 90 mm diameter and 200 mm height was used for the experiments. The light source was a 250 W mercury lamp (165 mm body length and 80 mm arc length) with wavelength range of 280–400 nm and the maximum emission of 365 nm. The lamp was installed centrally and immersed in the solutions. This configuration allows a homogeneous irradiation and perfect reflection for the beams contacting the reactor wall. At the beginning of each experiment, the ultrasound source (28 kHz, 60 W), located outside the bottom of the reactor, was working for 5 min, propagating waves in the reaction media in order to break up any particle cluster and providing homogeneous TiO_2 nanoparticle suspensions. During experiments, temperature was maintained constant by means of a stainless steel water-flow jacket from a thermostat bath.

To run experiments, a solution (1 L) containing the specified concentration of a Ni(II) salt and NA was prepared and was transferred into the reactor after pH adjustment by using either sulfuric acid or sodium hydroxide dilute solutions. Temperature was then set to the desired value. An amount of the catalyst particles (100 mg/L) was added,

and prior to light irradiation, the suspension was sonicated and then mixed for 30 min in the dark to ensure adsorption–desorption equilibria of the pollutants on TiO_2 particles. All the experiments were performed while the content was continuously mixed with a simple agitator. Initial pollutant concentration in the mixed solutions was 5 mg/L of Ni(II) and 10 mg/L of NA (unless mentioned otherwise). The selection of nickel and NA initial concentration was with respect to the feasible final concentration at the end of treatments being close to the permissible limit for discharge into surface water: 2 and 0.06 mg/L for Ni(II) and NA, respectively (WHO 2008). According to a report, the NA concentration frequently found in electroplating, dyeing and textile wastewaters is within 0.1–300 mg/L (Nesterenko-Malkovskaya *et al.* 2012).

To follow the reaction progress, 2 mL samples (at least two samples) were withdrawn each time, and after vigorous centrifuging to separate nanoparticles, were divided into 1 mL samples for analyzing Ni(II) and naphthalene content.

Analytical method

The concentration of Ni(II) and NA was determined from their absorption in the spectra obtained by a UV-vis spectrophotometer (Jasco, V-630, Japan). For Ni(II) ion, colorimetry at $\lambda_{max} = 568$ nm was performed using PAN color reagent as a standard method (Clesceri *et al.* 1998). Accordingly, the best conditions for the formation of Ni(II) complex were obtained by adding 2.5 mL of 1.0% Triton X-100 in water solution, 2 mL of buffer solution (pH 8.5), 1.0 mL of 0.01% PAN solution in ethanol, together with 1 mL of collected sample, all added into a 10 mL standard flask and making up to the marked level with deionized water. The NA analysis was performed from the change in the absorbance at its maximum wavelength of 275 nm (Mahmoodi & Sargolzaei 2014). Using these analysis procedures, the removal efficiency (*RE*) at any time was obtained from:

$$RE = \frac{[C]_0 - [C]_t}{[C]_0} \times 100 \quad (1)$$

where $[C]_0$ and $[C]_t$ denote initial and an appropriate time concentrations of a pollutant species, Ni(II) or NA.

As a representative of DO, the amount of H_2O_2 present was measured by colorimetry method with iodide. Briefly, 0.2 mL of diluted solution was mixed with 1.6 mL deionized water, 0.1 mL 1 M potassium iodine, and 0.1 mL 1 M sodium acetate buffer containing a few drops of ammonium dimolybdate as catalyst for the oxidation of I^- by H_2O_2 to I_3^-. The absorbance of solutions was measured by the UV-vis spectrophotometer at $\lambda_{max} = 360$ nm (Diesen & Jonsson 2014).

The separated TiO_2 particles, after process utilization, were washed with deionized water and then were dried at room temperature in a dark chamber. These particles as well as pure TiO_2 particles (before usage) were characterized in different ways.

RESULTS AND DISCUSSION

Reduction of Ni(II) ions

In preliminary experiments, the reduction of sole Ni(II) ions, originating from nitrate or sulfate salts, within concentration of 5–20 mg/L and with the conventional pH range of 7.5–9.5 (Saien *et al.* 2014; Saien & Azizi 2015), was examined. Titania photocatalyst concentration was fixed at 100 mg/L and temperature (*T*) was set within 20 to 40 °C. Under conditions of pH = 9.5 and $T = 35$ °C, removal efficiencies of 71.4% and 77.2% were achieved with 5 mg/L initial concentration of Ni(II), originating from nitrate and sulfate salts, respectively (Figure 1).

Counter-anions can play a role of scavenging photo-generated hydroxyl radicals and the photo-generated holes and consequently enhance the photocatalytic reduction of metal ions, according to the following reactions

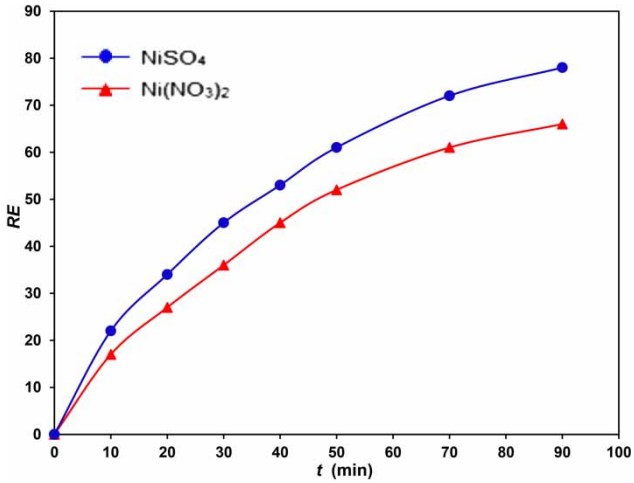

Figure 1 | Effect of the salt source on the removal efficiency of Ni(II) after 90 min; $[Ni(II)]_0 = 5$ mg/L, pH = 9.5 and $T = 35$ °C.

(Burns *et al.* 1999):

$$TiO_2 \xrightarrow{hv} e^- + h^+_{vb} \quad (2)$$

$$Ni(II) + 2e^- \rightarrow Ni^0 \quad (3)$$

$$SO_4^{2-} + h^+_{vb} \rightarrow SO_4^{\bullet -} \quad (4)$$

$$SO_4^{2-} + {}^{\bullet}OH \rightarrow SO_4^{\bullet -} + OH^- \quad (5)$$

or alternatively:

$$NO_3^- + h^+_{vb} \rightarrow NO_3^{\bullet} \quad (6)$$

$$NO_3^- + {}^{\bullet}OH \rightarrow NO_3^{\bullet} + OH^- \quad (7)$$

Thus, the capture of holes by counter-anions causes the photo-promoted electrons on the CB to become more readily available for nickel reduction, inhibiting electron–hole recombination. The interaction between counter anions and titania particles leads to the easier adsorption of nickel cations and therefore more ion reduction. It is noteworthy that the influence of ion strength on the electrostatic interaction between ions and the catalyst surface follows the charge-density order, presented in the Hofmeister series. Since SO_4^{2-} anion has a higher ionic strength compared to NO_3^-, higher ion reduction will correspond to nickel sulfate. In a previous study on the photocatalytic treatment of metal ions and organic pollution by sulfuric acid-modified titania (SO_4^{2-}/TiO_2) particles, it was reported that sulfate ions improve the photocatalytic activity (Samantaray *et al.* 2003). Meanwhile, NO_3^- ions from nitrate salt may convert to nitrite ions, NO_2^-, due to photolysis, and in turn generate H_2O_2 molecules, which is a disturbing factor in the reduction of Ni(II) ions (Tzou *et al.* 2008).

Figure 2(a) shows significant enhancement in the nickel *RE* with pH variation from 7.5 to 9.5. It is well known that TiO_2 surface is negatively charged at pHs more than pH_{PZC} (point of zero charge) which is within 6.7–7.5 for P-25 TiO_2 (Wang *et al.* 2004). Increase in the solution pH causes the TiO_2 surface to find negative charge, leading to higher Ni(II) ion adsorption. Thus, the nickel reduction increased from 23.6 to 69.8% for nickel sulfate and from 17.6 to 62.1% for nickel nitrate when pH was increased from 7.5 to 9.5, respectively. In addition, $Ni(OH)_2$ formation and precipitation occurs under high alkaline pHs (Lin & Rajeshwar 1997; Shirzad-Siboni *et al.* 2012; Gutha *et al.* 2015). Accordingly, for treatments with just the photocatalytic process, the pH of solutions was limited to maximum 9.5.

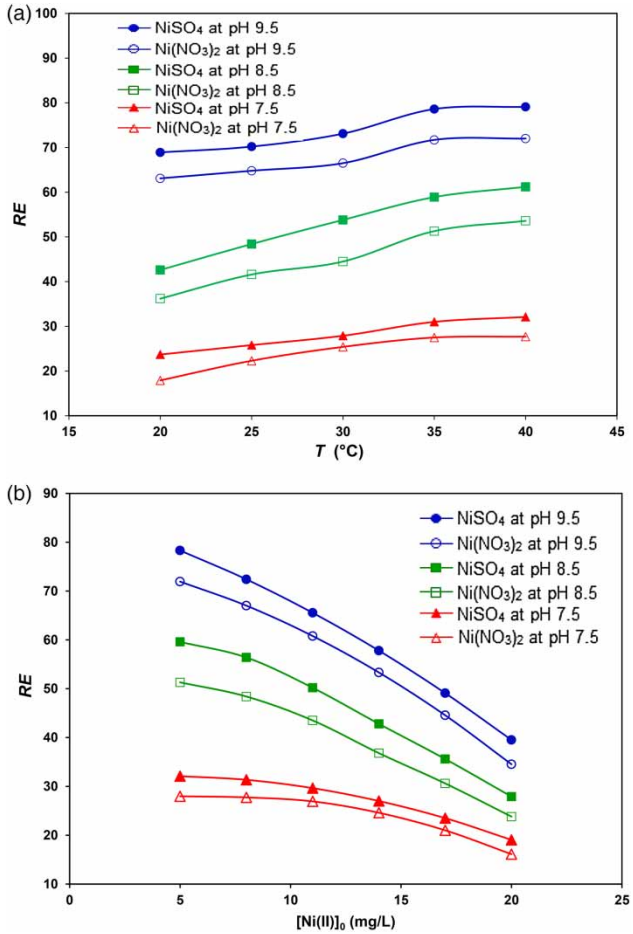

Figure 2 | Removal efficiency of Ni(II), after 90 min, versus temperature with $[Ni(II)]_0 = 5$ mg/L (a) and versus nickel initial concentration under the same conditions and $T = 35$ °C (b).

Figure 2(a) also demonstrates that temperature enhances the nickel *RE*; however, amounts more than 35 °C, do not provide much variation, which may be due to the low level activation energy in the photocatalytic reactions (Saien & Azizi 2015).

The influence of nickel initial concentrations is shown in Figure 2(b). Obviously, *RE* decreases with nickel concentration. This is because the catalyst surface becomes highly covered at high nickel concentrations and the light reaching the catalyst surface is diminished. Therefore, electron–hole formation becomes severe.

Moreover, kinetic studies revealed a pseudo-first-order kinetics for photocatalytic reduction of Ni(II) under conditions of $[Ni(II)]_0 = 5$ mg/L, pH = 9.5 and $T = 35$ °C, for both used salts. The rate constants were obtained as 1.81×10^{-3} and 1.63×10^{-3} 1/min for sulfate and nitrate salts, respectively.

Simultaneous reduction of Ni(II) and degradation of NA

In this step, preliminary experiments on adsorption of Ni(II) and NA on TiO_2 particles (100 mg/L) were performed in darkness. Adsorption of Ni(II) ions, originating from both the salts, on TiO_2 nanoparticles was measured in the presence and absence of NA (10 mg/L). The percentage of adsorption after a typical 60 min time is shown in Figure 3. The surface charge of TiO_2 particles in the used solution is slightly negative under natural solution pH of 7.5, which favors the electrostatic attraction between the opposite charged TiO_2 particles and Ni(II) cations. This adsorption is decreased in the presence of NA due to competition between Ni(II) and NA species. NA is rather a neutral compound and its adsorption is favored around neutral pHs (Lair *et al.* 2008). On the other hand, NA adsorption is enhanced in the presence of Ni(II), so that 13.2% NA adsorption increases to 15.4% when accompanied by either of the nickel salts. The 'salting-out' effect can be the major reason for this observation in the mixture (Lair *et al.* 2008). An increase in the ionic strength due to the presence of nickel salts causes a decrease in the solubility of NA and the resulting adsorption of hydrophobic NA species on the surface of TiO_2 particles.

In the photocatalytic process with light emission, Figure 4 shows that, in contrast with darkness, the *RE* for Ni(II) reduction, from either of the salts, is enhanced upon coupling with NA degradation, and reaches 52.7% and 47.8% at pH 7.5. *RE*s for Ni(II) reduction, in the absence of NA and under the same conditions were 25.8% and 22.3% for sulfate and nitrate salts respectively. This positive performance can be attributed to the consumption of photo-generated holes in NA degradation and inhibition of the electron–hole recombination. The photo-promoted CB electrons, generated by TiO_2 particles under UV irradiation, become more readily available for Ni(II) ions and hence an easier reduction will be established. The NA degradation is also enhanced in the presence of nickel ions. The *RE* of NA was raised from 36.5% to 50.6% with nickel sulfate and to 48.3% with nickel nitrate. The stronger NA adsorption in the presence of nickel salts can be considered to be due to the salting-out effect. The enhancement of Ni(II) reduction and NA degradation implies a synergism for the process.

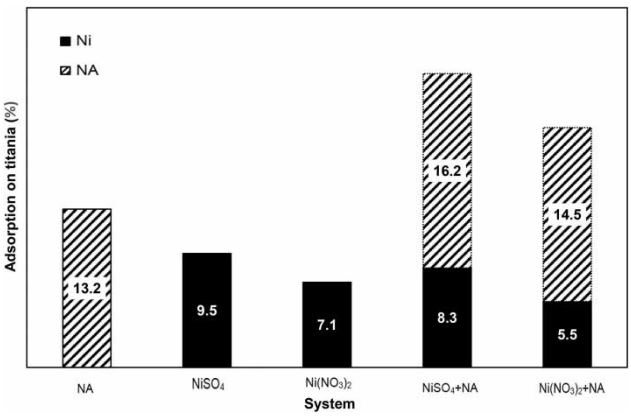

Figure 3 | Ni(II) and NA adsorption on TiO_2 particles in darkness for different systems after 60 min; $[Ni(II)]_0 = 5$ mg/L, $[NA]_0 = 10$ mg/L, pH = 7.5 and $T = 25$ °C.

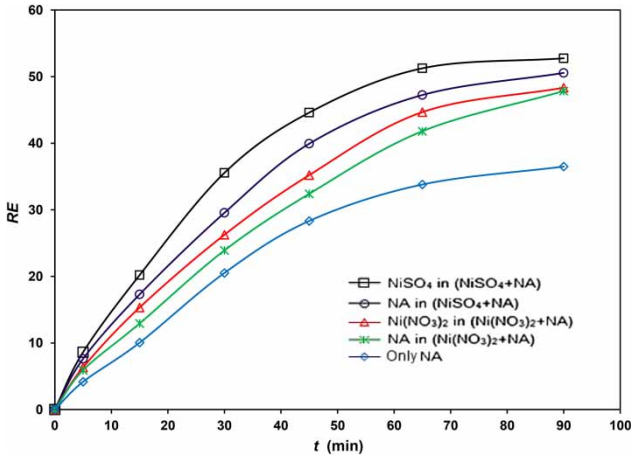

Figure 4 | Removal efficiencies for different investigated processes; $[Ni(II)]_0 = 5$ mg/L, $[NA]_0 = 10$ mg/L, pH = 7.5 and $T = 25$ °C.

It is worth noting that similar to a previous report on photocatalytic degradation of aniline with TiO_2 particles (Wang *et al.* 2009), a surface charge transfer complex can form between opposite charges of Ti^{4+} and O^{2-} from the TiO_2 structure and C^- and H^+ from NA, respectively (Rei *et al.* 2002). Based on these assumptions, for which a simple scheme is illustrated in Figure 5, the formed NA-TiO_2 surface species can be photo-excited upon light absorption and initiate a direct electron transfer into the CB of TiO_2 particles. The photo-induced electrons, injected into CB, can easily be trapped by Ni(II) ions which act as electron acceptor and accelerate NA conversion to a radical cation ($NA^{\bullet+}$). Subsequently, intermediates such as 1-naphthol, 1,2-benzenedicarboxaldehyde, 1,4-naphthoquinone, alkyl phthalates and some others are formed by a series of electron transfer mineralization mechanisms (Wang *et al.* 2009). The *in situ* formation of Ni/TiO_2 and NiO/TiO_2 nanocomposites is one advantage of this process. This product can be used as an efficient photocatalyst in degradation of pollutants under UV or solar irradiations (Sharma & Lee 2015).

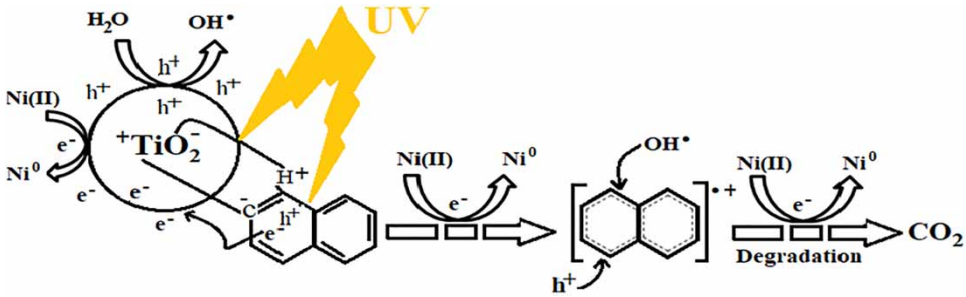

Figure 5 | Schematic presentation of the simultaneous photocatalytic reduction of Ni(II) and oxidation of NA with TiO_2 particles.

The Fourier transform infrared (FTIR, Perkin-Elmer, Spectrum 65, USA) spectra of TiO_2 powders, before and after usage, are shown in Figure 6(a). The broad peaks centered between 3,600 and 3,400 cm^{-1} and at 1,630 cm^{-1} correspond to the stretching vibrations of O-H groups and the bending vibrations of the adsorbed water molecules, respectively. The peak appearing below 1,200 cm^{-1} corresponds to Ti-O-Ti vibrations. Further, in Ni/TiO_2 composite, a weak band is observed at 2,925 cm^{-1}, which can be due to the presence of Ni over the TiO_2 surface (Begum *et al.* 2008). Other bands at 1,713.8 cm^{-1} and 1,387.5 cm^{-1} are assigned to N-O in nitrate ions (Hankare *et al.* 2011) and the band between 1,450 and 1,350 cm^{-1} is assigned to S=O in sulfate ions (Samantaray *et al.* 2003). The other appeared peaks correspond to the adsorption of trace amounts of sulfate or nitrate anions on the surface of titania nanoparticles. Further, the peak at about 1,000 cm^{-1} can be assigned to Ti-O-C stretching bond (Pavia *et al.* 2009). It is significant that there is no strong peak, relevant to aromatic C-H and C-C stretching vibrations, within 2,800–3,000 cm^{-1} and 1,672–1,696 cm^{-1} regions, respectively. These confirm that adsorbed NA species on the TiO_2 surface are completely oxidized.

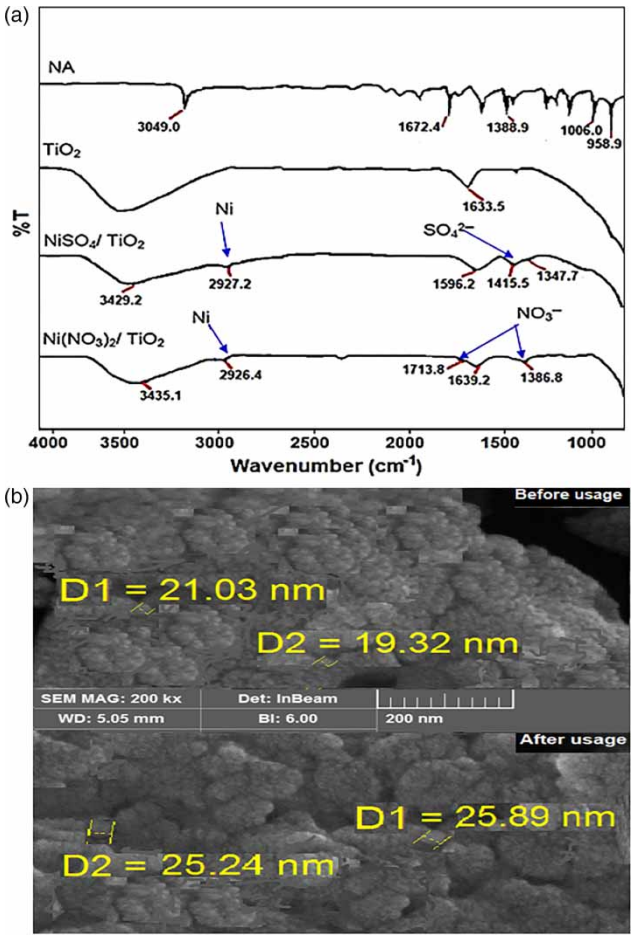

Figure 6 | FTIR spectra of NA and also TiO_2 particles before and after usage in simultaneous photocatalytic reduction of Ni(II) and degradation of NA (a), and SEM image of TiO_2 particles in the simultaneous photocatalytic treatment of $NiSO_4$ and NA, before and after usage (b); $[Ni(II)]_0 = 5$ mg/L, $[NA]_0 = 10$ mg/L, pH = 7.5 and $T = 25$ °C.

The scanning electron microscopy (SEM, Tescan, Mira 3, Czech Republic) was used to determine the morphology of the TiO_2 nanoparticles before usage and of collected and dried particles after usage. The SEM image (Figure 6(b)) reveals that the formed nanocomposite particles have regular and spherical shape after TiO_2 doping with nickel species (Ni^0 and NiO). The bigger found particle size (25.6 nm compared to 20.2 nm) is similar to a report for synthesizing mesoporous (Ni^{2+}/Ni^{3+})-TiO_2 particles with combined sol-gel and thermal decomposition methods (Rajendran *et al.* 2018). In a previous study using X-ray photoelectron spectroscopy to analyze used photocatalyst particles (Saien *et al.* 2014), the presence of nickel species on the titania surface (Ni^0 and NiO) was confirmed, because of immediate oxidation of metallic nickel.

In addition, the TiO_2 particles, before and after usage, were characterized by N_2 adsorption–desorption porosimetry using a BET analyzer (BELSORP, Mini II, Japan). The results, presented in Table 1, indicate that the average surface area and the average diameter of TiO_2 particles before usage agree with the manufacturer's reported values ('Materials and methods' section). Meanwhile, the collected

Table 1 | BET surface analysis of TiO_2 nanoparticles in the photocatalytic treatment of $NiSO_4$ and NA

Sample	Surface area (m^2/g)	Average diameter$_{BET}$ (nm)	Pore volume (cm^3/g)	Pore size (nm)
TiO_2 before usage	50 ± 15	21	0.17	16.4
TiO_2 after usage	43 ± 10	26	0.24	20.2

TiO_2 particles after usage consistently have less surface area and large pores, compared with initial particles, respectively. These kinds of changes have also been reported for nanocomposites such as Ag/TiO_2 and NiO/TiO_2, synthesized by methods other than photocatalytic reduction (Rajendran *et al.* 2018; Saravanan *et al.* 2018).

The effect of pH on the photocatalytic treatment is shown in Figure 7(a) typically for nickel sulfate. The results show that nickel reduction increases steadily with pH while the NA oxidation increases up to pH of about 8 and then decreases. By changing the solution pH, the photocatalyst surface charge is altered and the NA and Ni(II) adsorption is changed. The TiO_2 surface is positively charged in acidic solutions and negatively charged in alkaline solutions with respect to the most reported pH_{PZC} of P25 TiO_2, which is within 6.7–7.5 (Wang *et al.* 2004). The influence of pH on NA degradation can be interpreted by radical reactions. Under acidic pHs, the formation of $^{\bullet}OH$ radical is unstable, and by increasing pH, more radicals are produced, giving more NA degradation. As documented (Bekbolet & Balcioglu 1996), by NA degradation, at pHs higher than 8, carbonate ions (CO_3^{2-}) are formed which may act as $^{\bullet}OH$ scavenger, leading to lower NA degradation,

$$OH^- \xrightarrow{h\nu} {}^{\bullet}OH \quad (8)$$

$$CO_3^{2-} + {}^{\bullet}OH \rightarrow CO_3^{\bullet -} + OH^- \quad (9)$$

The respective average Ni(II) and NA *RE*s show an ascending and then a flat variation with pH. The highest

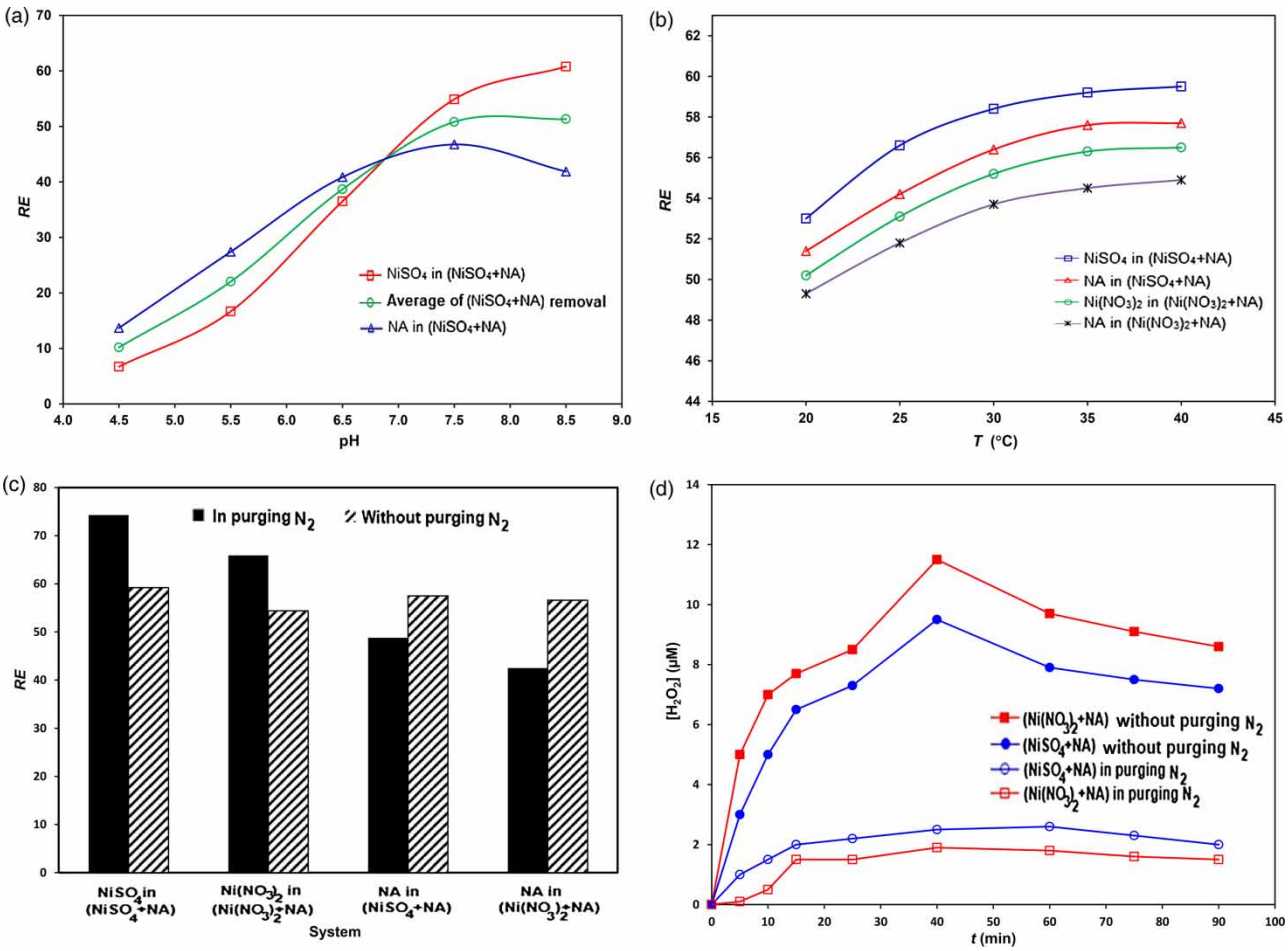

Figure 7 | Removal efficiencies after 90 min treatments, $[Ni(II)]_0 = 5$ mg/L, $[NA]_0 = 10$ mg/L: effect of pH at $T = 25$ °C (a), effect of temperature at pH = 7.5 (b), effect of purging nitrogen gas on *RE*s (c), and comparison of H_2O_2 generation (d) under given conditions.

average *RE* was found at pH around 7.5 for both the sulfate and nitrate nickel salts.

Investigation on temperature effect (Figure 7(b)) revealed that nickel reduction and NA degradation increase with temperature increase from 20 to about 35 °C and then remain almost constant perhaps due to a temperature disfavor effect on their adsorption. An average enhancement of about 12.4% was achieved for treatments below pH 7.5 after 90 min. Temperature helps the photocatalytic reactions to compete with the non-favorable electron–hole pair recombination; however, the low level activation energy of photocatalytic reactions gives a small temperature effect (Saien & Azizi 2015). Temperature of 35 °C can suit operations, giving 58.4% average *RE* (59.2% for Ni(II) and 57.5% for NA) for sulfate and 55.5% average *RE* (54.5% for Ni(II) and 56.6% for NA) for nitrate salts. In addition to the reasons given in the section on just Ni(II) reduction, more electron–hole recombination is expected under a low level of metal reduction, which in turn gives lower NA degradation.

The role of ROS in the process was investigated by continuous nitrogen gas purging into solutions. Figure 7(c) shows that 61.5% average *RE* (74.3% for Ni(II) and 48.8% for NA) and 54.2% average *RE* (65.9% for Ni(II) and 42.5% for NA) were obtained for sulfate and nitrate salts, respectively, and a higher reduction of Ni(II) ion and a lower oxidation of NA occurred. It has been reported that reduction of metals, with low reduction potential, is difficult with DO due to competition between metal ions and DO to attract electrons in the CB of TiO_2 (Yang *et al.* 2012). Meanwhile the efficiency of NA oxidation is diminished under these conditions. DO acts as an effective electron acceptor to extend the hole's lifetime and also may be involved in the formation of ROS, such as H_2O_2 molecule, which contribute in photocatalyst reactions of NA degradation (Nosaka & Nosaka 2017).

H_2O_2 is a rather stable molecule of the ROS, and the amount of this species was measured easily with iodide method (Nosaka & Nosaka 2017) either with or without nitrogen purging. The results in Figure 7(d) show that H_2O_2 formation highly increases at initial times and then tends to decrease due to its consumption in NA oxidation. As expected, H_2O_2 formation is very low in continuous nitrogen purging due to the absence of DO.

Kinetic study

Owing to practical applications, the kinetics of photocatalytic reactions was investigated under mild mentioned operating conditions and during 90 min treatment. Results show that Ni(II) photocatalytic reduction and NA degradation in the mixed solution are well described by pseudo-first-order kinetic models as $\ln[C_0/C_t] = kt$ where C_0, C_t and k are the initial concentration and at any time, t, of Ni(II) or NA, and the kinetic rate constant, respectively. The rate constants as well as the coefficient of determination (R^2) for different investigated cases are listed in Table 2.

Table 2 | The rate constants of Ni(II) reduction and NA oxidation; $[Ni(II)]_0 = 5$ mg/L, $[NA]_0 = 10$ mg/L, pH = 7.5, $T = 35$ °C and during 90 min treatments

Process	k (1/min)	R^2
$Ni(NO_3)_2$	0.0027	0.970
$NiSO_4$	0.0037	0.952
NA	0.0054	0.983
$Ni(NO_3)_2$ in $(Ni(NO_3)_2 + NA)$	0.0080	0.983
$NiSO_4$ in $(NiSO_4 + NA)$	0.0086	0.992
NA in $(Ni(NO_3)_2 + NA)$	0.0075	0.997
NA in $(NiSO_4 + NA)$	0.0082	0.993

Energy consumption analysis

Among several factors in selecting a method for pollutants treatment, economics is vital. In this regard, electrical energy consumption, E_{EC}, has the main contribution in the photochemical processes. Here, E_{EC} can be calculated according to the proposal of the Photochemistry Commission of the International Union of Pure and Applied Chemistry (IUPAC) for the first-order reactions as (Bolton *et al.* 2001):

$$E_{EC} = \frac{1000Pt}{60V\log[C_0/C_t]} \tag{10}$$

where P is the electric power (kW) of the photochemical system, V is the solution volume (L) in the reactor and t is the reaction duration time (min). In order to take into account the impact of reaction temperature variation on the E_{EC} calculations, Equation (10) can be given as the following equation, noting that the constant $\ln[C_0/C_t]/t$ represents the rate constant k (1/min):

$$E_{EC} = \frac{38.4P}{Vk} \tag{11}$$

Based on obtained rate constants, the electrical energy related to the photocatalytic removal of each pollutant

Table 3 | The performance of the used photoatalytic process for simultaneous Ni(II) reduction and NA oxidation in comparison with other reported processes

Photocatalytic process	[Ni(II)] or [NA] (mg/L)	[TiO_2] (mg/L)	pH	Lamp power (W)	*t* (min)	Accompanied reagent	*RE* (%)	E_{EC} (kWh/m^3)	*PE* 1/[(kWh/m^3) (mg/L)]	Reference
$Ni(NO_3)_2 + TiO_2$	15	1,000	7.0	125	120	–	55.0	720.9	7.63×10^{-5}	Karimi *et al.* (2013)
$Ni(NO_3)_2 + ZnO$	5	1,000	7.0	125	120	–	41.0	1,091.1	3.76×10^{-5}	Kabra *et al.* (2007)
$NiSO_4 + TiO_2$	5	100	7.5	250	90	–	32.1	2,594.6	1.24×10^{-4}	This work
$Ni(NO_3)_2 + TiO_2$	5	100	7.5	250	90	–	27.9	3,555.5	7.85×10^{-5}	This work
$NiSO_4 + TiO_2$	5	100	7.5	250	90	NA, 10 mg/L	59.2	1,116.3	5.30×10^{-4}	This work
$Ni(NO_3)_2 + TiO_2$	5	100	7.5	250	90	NA, 10 mg/L	54.5	1,199.8	4.54×10^{-4}	This work
$NA + TiO_2$	10	100	7.5	250	90	$Ni(NO_3)_2$, 5 mg/L	56.6	1,280.1	4.42×10^{-4}	This work
$NA + TiO_2$	10	100	7.5	250	90	$NiSO_4$, 5 mg/L	57.5	1,170.7	4.91×10^{-4}	This work
$NA + TiO_2$	10	100	7.5	250	90	–	36.5	1,777.8	2.50×10^{-4}	This work

under dominant conditions was obtained as 1,116.3 and 1,199.8 kWh/m^3 for Ni(II) and 1,170.7 and 1,280.1 kWh/m^3 for NA, when sulfate and nitrate nickel salts were used in the mixtures, respectively. The calculated values for simultaneous treatments are less than the electrical quantities required for treatment of each pollutant individually (Table 3). Considering the current electrical energy (industrial sector) price in the US market as 0.0702 US$/kWh in 2018 (US EIA 2018), the electrical energy cost relating to the above four electrical energy amounts is estimated as 78.4, 84.2 and 82.2, 89.9 US$/m^3, respectively.

Finally, a valid criterion of process efficiency (*PE*), corresponding to *RE* when assigned to unit electrical energy consumption and the employed photocatalyst dosage, can be introduced as:

$$PE = \frac{RE}{E_{EC} \times [TiO_2]} \tag{12}$$

This criterion reflects the efficiency, achieved with respect to the level of energy consumption as well as the catalyst dosage. Accordingly, the effect of temperature and the reaction progress are involved in *PE* via the E_{EC} parameter.

The removal efficiencies as well as other described criteria are listed in Table 2 in comparison with other previously reported studies on photocatalytic reduction of Ni(II). The pseudo-first-order reactions are relevant under corresponding operating conditions. It is seen that despite nearly the same order of E_{EC}, the *PE* values for nickel ion, in this work, are about one order of magnitude higher than those of referenced works. Effective light in the used photoreactor and the synergism action of the reduction/degradation process are the main reasons for this very significant preference.

CONCLUSIONS

In this study the enhanced photocatalytic reduction of Ni(II) was demonstrated when simultaneously performed with naphthalene degradation and using a low dosage of titania nanoparticles. The photocatalyst hole consumption by naphthalene causes lowering of the electron–hole recombination and acceleration of the electron trapping by Ni(II) ions. Further, the formed naphthalene-TiO_2 species can be photo-excited upon light absorption and provide a direct electron transfer into Ni(II) ions. Confirming the results, the TiO_2 particles before and after usage were characterized by means of several techniques and it was found that average particles size, after usage, was increased due to nickel doping while the pore size was increased. The other important findings were: (i) the optimum mild operating conditions were pH 7.5 and 35 °C; (ii) under pertinent conditions, the removal efficiency of Ni(II) ions, for both the used salts, was about twice that in the absence of naphthalene; (iii) there appears to be more opportunity for the reduction of Ni(II) ions when the sulfate salt is used, compared with nitrate salt, individually or simultaneously; (iv) nitrogen purging in the samples confirmed the favorable DO role in naphthalene degradation and negative role in nickel reduction; (v) the Ni(II) ion reduction and naphthalene degradation obey pseudo-first-order kinetic reactions; (vi) electrical energy consumption analysis showed a relatively low required energy for the simultaneous treatment systems in comparison with individual treatments under the

same conditions; and (vii) based on different criteria, including economic parameters, the significant preference of the process was revealed.

ACKNOWLEDGEMENTS

The authors wish to thank the university authorities for providing the financial support to carry out this project. The authors also acknowledge Evonik Industries for supplying TiO_2 (P-25) as a gift to our research group.

REFERENCES

Akhtar, N., Iqbal, J. & Iqbal, M. 2004 Removal and recovery of nickel(II) from aqueous solution by loofa sponge-immobilized biomass of *Chlorella sorokiniana*: characterization studies. *Journal of Hazardous Materials* **108**, 85–94.

Alqadami, A. A., Naushad, M., Alothman, Z. A. & Ghfar, A. A. 2017 Novel metal-organic framework (MOF) based composite material for the sequestration of U(VI) and Th(IV) metal ions from aqueous environment. *ACS Applied Materials and Interfaces* **9**, 36026–36037.

Aman, N., Mishra, T., Hait, J. & Jana, R. K. 2011 Simultaneous photoreductive removal of copper (II) and selenium (IV) under visible light over spherical binary oxide photocatalyst. *Journal of Hazardous Materials* **186**, 360–366.

Ashour, I., Abu Al-Rub, F. A., Sheikha, D. & Volesky, B. 2008 Biosorption of naphthalene from refinery simulated wastewater on blank alginate beads and immobilized dead algal cells. *Separation Science and Technology* **43**, 2208–2224.

Barakat, M. A. 2004 New trends in removing heavy metals from industrial wastewater. *Journal of Membrane Science* **4**, 361–377.

Begum, N. S., Ahmed, H. M. F. & Gunashekar, K. R. 2008 Effects of Ni doping on photocatalytic activity of TiO_2 thin films prepared by liquid phase deposition technique. *Bulletin of Materials Science* **31**, 747–751.

Bekbolet, M. & Balcioglu, I. 1996 Photocatalytic degradation kinetics of humic acid in aqueous TiO_2 dispersions: the influence of hydrogen peroxide and bicarbonate ion. *Water Science and Technology* **34**, 73–80.

Besharat, E. 2010 *Electroplating Engineering*. Designer Publisher, Tehran, Iran.

Blake, D. M., Webb, D. J., Turchi, C. & Magrini, K. 1991 Kinetic and mechanistic overview of titania photocatalyzed oxidation reactions in aqueous solution. *Solar Energy Materials and Solar Cells* **24**, 584–593.

Bolton, J. R., Bircher, K. G., Tumas, W. & Tolman, C. A. 2001 Figures-of-merit for the technical development and application of advanced oxidation technologies for both electric- and solar-driven systems. *Pure and Applied Chemistry* **73**, 627–637.

Burns, R. A., Crittenden, J. C., Hand, D. W., Selzer, V. H., Sutter, L. L. & Salman, S. M. 1999 Effect of inorganic ions in the heterogenous photocatalysis of trichloroethene. *Journal of Environmental Engineering* **125**, 77–85.

Caicedo, M. 2008 Analysis of metal ion-induced DNA damage, apoptosis, and necrosis in human (Jurkat) T-cells demonstrates Ni^{2+} and V^{3+} are more toxic than other metals: Al^{3+}, Be^{2+}, Co^{2+}, Cr^{3+}, Cu^{2+}, Fe^{3+}, Mo^{5+}, Nb^{5+}, Zr^{2+}. *Journal of Biomedical Materials Research Part A* **86**, 905–913.

Chen, D. & Ray, A. K. 2001 Removal of toxic metal ions from wastewater by semiconductor photocatalysis. *Chemical Engineering Science* **56**, 1561–1570.

Clesceri, L. S., Greenberg, A. E. & Eaton, A. D. 1998 *Standard Methods for the Examination of Water and Wastewater*. American Public Health Association/American Water Works Association/Water Environment Federation, Washington, DC, USA.

Diesen, V. & Jonsson, M. 2014 Formation of H_2O_2 in TiO_2 photocatalysis of oxygenated and deoxygenated aqueous systems: a probe for photocatalytically produced hydroxyl radicals. *The Journal of Physical Chemistry C* **118**, 10083–10087.

Doan, H. D. & Saidi, M. 2008 Simultaneous removal of metal ions and linear alkyl benzene sulfonate by combined electrochemical and photocatalytic process. *Journal of Hazardous Materials* **158**, 557–567.

Gutha, Y., Munagapati, V. S., Naushad, M. & Abburi, K. 2015 Removal of Ni(II) from aqueous solution by *Lycopersicum esculentum* (Tomato) leaf powder as a low-cost biosorbent. *Desalination and Water Treatment* **54**, 200–208.

Gutierrez, R., Flores, S., Rios, O. & Valenzuela, M. 2008 Simultaneous Cr(VI) reduction and naphthalene oxidation in aqueous solutions by UV/TiO_2. *Materials Research Society Symposium Proceedings* **1045**, 1–5.

Hankare, P. P., Patil, R. P., Jadhav, A. V., Pandav, R. S., Garadkar, K. M., Sasikala, R. & Tripathi, A. K. 2011 Synthesis and characterization of nanocrystalline Ti-substituted Zn ferrite. *Journal of Alloys and Compounds* **509**, 2160–2163.

Joshi, K. M., Patil, B. N., Shirsath, D. S. & Shrivastava, V. S. 2011 Photocatalytic removal of Ni(II) and Cu(II) by using different semiconducting materials. *Advances in Applied Science Research* **2**, 445–454.

Kabra, K., Chaudhary, R. & Sawhney, R. L. 2007 Effect of pH on solar photocatalytic reduction and deposition of Cu(II), Ni(II), Pb(II) and Zn(II): speciation modeling and reaction kinetics. *Journal of Hazardous Materials* **149**, 680–685.

Karimi, B., Rajaei, M. S., Habibi, M. & Abdollahy, M. 2013 Effect of UV/H_2O_2 advanced oxidation processes for the removal of naphthalene from the water solution. *Arak Medical University Journal* **16**, 50–64.

Lair, A., Ferronato, C., Chovelon, J. M. & Herrmann, J. M. 2008 Naphthalene degradation in water by heterogeneous photocatalysis: an investigation of the influence of inorganic anions. *Journal of Photochemistry and Photobiology A: Chemistry* **193**, 193–203.

Lin, W. & Rajeshwar, K. 1997 Photocatalytic removal of nickel from aqueous using UV irradicated TiO_2. *Journal of Electrochemical Society* **97**, 2–20.

Mahmoodi, V. & Sargolzaei, J. 2014 Photocatalytic abatement of naphthalene catalyzed by nanosized TiO_2 particles: assessment of operational parameters. *Theoretical Foundations of Chemical Engineering* **48**, 656–666.

Naushad, M., Ahamad, T., Al-Maswari, B. M., Abdullah Alqadami, A. & Alshehri, S. M. 2017 Nickel ferrite bearing nitrogen-doped mesoporous carbon as efficient adsorbent for the removal of highly toxic metal ion from aqueous medium. *Chemical Engineering Journal* **330**, 1351–1360.

Nesterenko-Malkovskaya, A., Kirzhner, F., Zimmels, Y. & Armon, R. 2012 *Eichhornia crassipes* capability to remove naphthalene from wastewater in the absence of bacteria. *Chemosphere* **125**, 124–128.

Nosaka, Y. & Nosaka, A. Y. 2017 Generation and detection of reactive oxygen species in photocatalysis. *Chemical Reviews* **117**, 11302–11336.

Pavia, D. L., Lampman, G. M., Kriz, G. S. & Vyvyan, J. A. 2009 *Introduction to Spectroscopy*. Saunders Golden, Western Washington University Bellingham, Washington.

Rajendran, S., Manoj, D., Raju, K., Dionysiou, D. D., Naushad, M., Gracia, F., Cornejo, L., Gracia-Pinilla, M. A. & Ahamad, T. 2018 Influence of mesoporous defect induced mixed-valent NiO (Ni^{2+}/Ni^{3+})-TiO_2nanocomposite for non-enzymatic glucose biosensors. *Sensors and Actuators, B: Chemical* **264**, 27–37.

Rei, S., Krumm, H., Niklewski, A. & Staemmler, V. 2002 The adsorption of acenes on rutile TiO_2: a multi-technique investigation. *Journal of Chemical Physics* **116**, 7704–7713.

Saien, J. & Azizi, A. 2015 Simultaneous photocatalytic treatment of Cr(VI), Ni(II) and SDBS in aqueous solutions: evaluation of removal efficiency and energy consumption. *Process Safety and Environmental Protection* **95**, 114–125.

Saien, J., Azizi, A. & Soleymani, A. R. 2014 Optimized photocatalytic conversion of Ni(II) ions with very low titania nanoparticles at different temperatures; kinetics and energy consumption. *Separation and Purification Technology* **134**, 187–195.

Samantaray, S. K., Mohapatra, P. & Parida, K. 2003 Physico-chemical characterisation and photocatalytic activity of nanosized SO_4^{2-}/TiO_2 towards degradation of 4-nitrophenol. *Journal of Molecular Catalysis A: Chemical* **198**, 277–287.

Saravanan, R., Manoj, D., Qin, J., Naushad, M., Gracia, F., Lee, A. F., Khan, M. M. & Gracia-Pinilla, M. A. 2018 Mechanothermal synthesis of Ag/TiO_2 for photocatalytic methyl orange degradation and hydrogen production. *Process Safety and Environmental Protection* **120**, 339–347.

Sharma, A. & Lee, B. 2015 Adsorptive/photo-catalytic process for naphthalene removal from aqueous media using in-situ nickel doped titanium nanocomposite. *Journal of Environmental Management* **155**, 114–122.

Shirzad-Siboni, M., Samadi, M. T., Yang, J. K. & Lee, S. M. 2012 Photocatalytic removal of Cr(VI) and Ni(II) by UV/TiO_2: kinetic study. *Desalination and Water Treatment* **40**, 77–83.

Tzou, M. T., Hsu, C. L., Chen, C. C., Chen, J. H., Wu, J. J. & Tseng, K. J. 2008 Influence of inorganic anion on Cr(VI) photoreduction in the presence of ferric ion. *Journal of Hazardous Materials* **156**, 374–380.

US EIA (Energy Information Administration 2018 *Independent Statistics and Analysis*. http://www.eia.doe.gov.

Wang, X., Pehkonen, S. O. & Ray, A. K. 2004 Removal of aqueous Cr(VI) by a combination of photocatalytic reduction and coprecipitation. *Industrial & Engineering Chemistry Research* **43**, 1665–1672.

Wang, N., Zhu, L., Huang, Y., She, Y., Yu, Y. & Tang, H. 2009 Drastically enhanced visible light photocatalytic degradation of colorless aromatic pollutants over TiO_2 via a charge transfer complex path: a correlation between chemical structure and degradation rate of the pollutants. *Journal of Catalysis* **266**, 199–206.

WHO 2008 *Guidelines for Drinking-Water Quality*. WHO, Geneva, Switzerland.

Yang, J. K., Lee, S. M., Farrokhi, M., Giahi, O. & Shirzad Siboni, M. 2012 Photocatalytic removal of Cr(VI) with illuminated TiO_2. *Desalination and Water Treatment* **46**, 375–380.

First received 7 September 2018; accepted in revised form 21 December 2018. Available online 17 January 2019